Proceedings of the 9th International Conference on Physical Modelling in Coastal Engineering (Coastlab24)

Delft, Netherlands, May 13-16, 2024

Conference Paper, DOI: 10.59490/coastlab.2024.687

GENERATION OF HIGHLY NONLINEAR WAVES IN A SHORT WAVE FLUME

MADS RØGE ELDRUP[1], THOMAS LYKKE ANDERSEN[2]

1 Dept. of the Built Environment, Aalborg University, Denmark, mrel@build.aau.dk

2 Dept. of the Built Environment, Aalborg University, Denmark, tla@build.aau.dk

ABSTRACT

The typical approach for generating nonlinear waves in physical models involves employing first- or second-order wave theory, requiring a large water depth at the wavemaker. When the prototype bathymetry shows a gentle slope, a large facility is required. However, practical constraints often make this unfeasible, leading to the use of steep transition slopes to obtain sufficient water depth at the generator. Incorporating a transition slope may generate unwanted free waves beyond the transition point, significantly impacting the wave parameters. The presence of these free waves causes the response of the tested structure to deviate from that found in the prototype. This paper offers guidelines for using transition slopes effectively while avoiding the generation of undesired free waves after the transition point.

KEYWORDS: Hybrid modelling, Transition slopes, Nonlinear waves, Wave transformation, Wave generation

1 INTRODUCTION

When studying wave transformation and hydraulic response in physical and numerical models, it is important to reproduce the conditions in nature as closely as possible. For coastal structures this often involves replicating highly nonlinear irregular waves in intermediate or shallow waters, and then the model layout demands particular attention, which forms the central focus of the present work. In physical models, the waves are usually produced using a moving paddle based on a given wavemaker theory. No analytical wavemaker solution exists for highly nonlinear irregular waves in intermediate and shallow water. Thus first- or second- order wavemaker theory is usually used, but this requires a quite large depth at the wavemaker to be valid, see Eldrup and Lykke Andersen (2019). For this reason, it is necessary to shoal the waves from a larger water depth in the physical models. In physical models the length of the foreshore is however limited by the length of the facility. Thus, replicating a prototype with a gentle uniform seabed and highly nonlinear waves is not possible unless a long flume is available. This is because the water depth needed at the wavemaker is determined by first- or second-order wavemaker theory to be valid. The same criteria apply to numerical models, but here the length of the foreshore is only restricted by the computational capacity. If the length of the physical facility is insufficient to replicate a prototype situation with a gentle seabed slope, alternative methods need to be employed to simulate the prototype conditions, as illustrated in Figure 1. The three alternative methods are:

Method 1: Hybrid modelling, where the output from a numerical model is used to drive the wavemaker in the physical model. The wave generation may then be based on shallow water wavemaker theory with a dispersion correction as proposed by Zhang et al. (2007);

Method 2: A steeper transition slope close to the wavemaker is used to give sufficient water depth for first- or second-order wavemaker theory to be valid;

Method 3: Using first- or second-order wavemaker theory in a depth where it is not valid.

Method 1 makes it possible to generate nonlinear intermediate and shallow water waves in a relatively short wave flume with the correct foreshore. The main limitation of that method is that wave breaking in the numerical model domain may not be correctly reproduced. Nonetheless, creating waves that break on the wavemaker is a situation that should be avoided if possible. During the last five years, Method 1 has been the preferred solution at Aalborg University for the generation of nonlinear waves in shallow water. Most other laboratories have preferred one of the other two alternatives.

Method 2 avoids free waves being generated at the wavemaker, but the wave transformation over a composite slope is quite different from a uniform slope. In the case of using a transition slope, Frostick et al. (2011) recommend that the length

of the foreshore after the transition slope is minimum 3-5 times the local wavelength as this ensures a correct wave shoaling and wave breaking on the foreshore. However, using a transition slope might also result in free waves being generated after the transition from a steep to a gentler slope, which has been shown by many researchers, such as Grue (1992) and Beji and Battjes (1993; 1994). The effect of these free waves has lately gained more attention, and studies have shown that they lead to the generation of freak waves, see Trulsen et al. (2020), Li et al. (2021) and Zhang et al. (2023). In the present paper further guidance on the use of transition slopes and the consequence on the generated waves is provided.

Method 3 uses a wavemaker theory outside its applicability range, and thus, free unwanted waves are generated at the wavemaker. The free waves cause deviations of the spectral energy along the foreshore as the free waves change from being out of phase with the bound waves at the paddle to being in phase at some distance from the wavemaker. These free waves can significantly influence the response of the structure, and Orszaghova et al. (2014) found that for their test cases, the overtopping volumes were between 25 and 83% higher when using first-order generation methods outside its applicability range compared to second-order generation methods. Eldrup and Lykke Andersen (2019) showed in a few examples the consequences of these free waves on the surface profile.

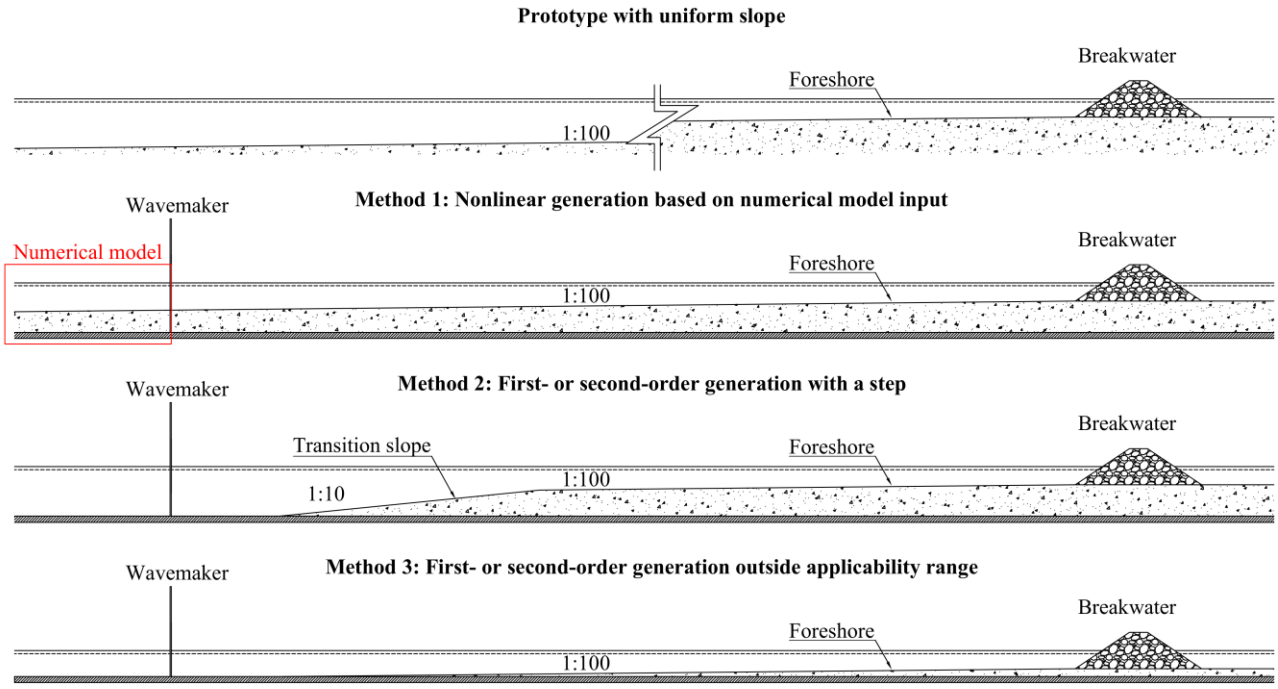

Figure 1. Sketch of prototype and three methods for wave generation in a short flume.

2 PRESENT STUDY

The present paper aims to provide improved guidance on wave generation of nonlinear waves in short flumes using transition slopes, as shown for Method 2 in Figure 1. It is well-established that Method 1 can closely replicate the prototype situation, provided that the used numerical model accurately represents the transformation and that waves do not break on the wavemaker. Method 3 generates unwanted free waves that result in deviations from the prototype conditions, which can lead to incorrect model responses and wave parameters along the foreshore. Consequently, this study aims to assess how the wave parameters achieved through Method 2 compared to those in the prototype situation with a uniform slope. This investigation will provide insights into the conditions under which Method 2 is suitable and when it is not. This will lead to guidance on maximum slope angles, transition depths and lengths of transition slopes.

The wave transformation is accurately reproduced in numerical models and thus the present study is solely based hereon. Firstly, regular waves are generated and analysed to describe the nonlinear wave transformation at a transition slope and the generation of free waves after the transition. Secondly, irregular waves are studied, and a larger range of seabed configurations are studied in order to describe when the unwanted free waves generated after the transition slope are significant.

In summary, this study seeks to provide guidance on generating highly nonlinear intermediate and shallow water waves within a relatively short wave flume by application of transition slopes, i.e. Method 2 in Figure 1.

3 REGULAR WAVES

The initial focus is on examining the transformation of regular waves shoaling along a transition slope to a horizontal

bathymetry. This investigation aims to show the processes involved when waves propagate across varying transition slopes and into a very gently sloping foreshore. In the present case the gentle foreshore is represented by a horizontal seabed which allows a separation of the free and bound wave components. Eldrup and Lykke Andersen (2020) numerically studied the shoaling and de-shoaling of regular waves, where they observed the release of free waves when the bathymetry slope changed. For gentle slopes the shoaling and de-shoaling of the wave components could be accurately described using stream function wave theory by Fenton and Rienecker (1980). However, as the bathymetry slope became steeper and the nonlinearity of the waves increased, the stream function wave theory deviated from the numerical results. During shoaling on steeper foreshores, the nonlinear waves get a steep front and gentler rear slope (positive atiltness). During de-shoaling on steeper foreshores free waves are released. Eldrup and Lykke Andersen (2020) also studied a bathymetry consisting of a 1:30 transition slope followed by a horizontal section. In this horizontal section, they observed that the released free wave components interacted and generated bound super and subharmonics. Their study on this layout was limited to one wave condition.

The release of free waves is studied numerically using the MIKE 3 Wave FM numerical model developed by DHI using the model domain shown in Figure 2. Regular waves are generated at a depth of h_{deep} = 1.5 m using a relaxation zone and stream function wave theory. The length of the relaxation zone is $2L_{deep}$ where L_{deep} is the linear wavelength in the generation zone. Different regular wave conditions are generated, i.e. wave heights H_{deep} = 0.05, 0.10 and 0.15 m and wave periods T = 2, 3, 4 and 5 s, see Table 1. After the relaxation zone, a horizontal section with a length of L_{deep} was used before the foreshore started. The foreshores tested were α = 1000, 100, 30 and 10. After the foreshore, a horizontal section was present with a length of $30L_{shallow}$, where $L_{shallow}$ is the linear wavelength at the depth $h_{shallow}$ = 0.5 m. After the horizontal section, a sponge layer with a width of $6L_{shallow}$ was used to absorb the waves. In total, 48 simulations with regular waves were performed.

The horizontal discretisation was $\Delta x = L_{shallow} / N_{cell}$ where N_{cell} is the number of cells per wavelength in the shallow end. For the shortest waves with T = 2 s, a horizontal resolution of N_{cell} = 100 was found adequate, while the remaining wave periods had N_{cell} = 150. The vertical resolution of the model was found to be adequate for all wave periods when using 10 layers (N_σ = 10). The varying time step was based on a maximum CFL criteria equal to 0.8. These values correspond well to the study by Andersen et al. (2024), where a convergence study was conducted comparing physical and numerical model tests with regular wave propagation for breaking and non-breaking conditions.

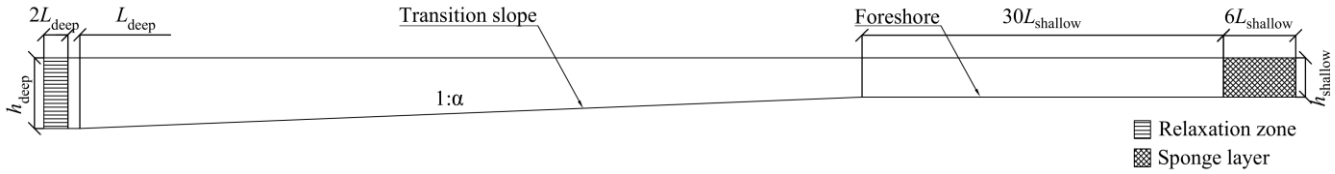

Figure 2. Setup of the numerical wave flume for regular wave tests.

Table 1 shows the tested wave parameters for each Case. The waves have a wave steepness from 0.1-2.4% calculated with the wave height at the generation point H_{deep} and the deep water wavelength $L_0 = T^2g/(2\pi)$ with g = 9.82 m/s^2. The waves are generated in transitional and shallow water as h_{deep}/L_0 varies between 0.01 and 0.24.

Table 1: Regular wave conditions.

Case	Deep water wave height, H_{deep} [m]	Wave period, T [s]	Deep water wave steepness, $s_0 = H_{deep}/L_0$ [%]	Relative water depth at generation, h_{deep}/L_0	Relative water depth at transition, $h_{shallow}/L_0$
RA1	0.05		0.8		
RA2	0.10	2	1.6	0.24	0.08
RA3	0.15		2.4		
RB1	0.05		0.4		
RB2	0.10	3	0.7	0.11	0.04
RB3	0.15		1.1		
RC1	0.05		0.2		
RC2	0.10	4	0.4	0.06	0.02
RC3	0.15		0.6		
RD1	0.05		0.1		
RD2	0.10	5	0.3	0.04	0.01
RD3	0.15		0.4		

Figure 3 shows at a given instance the variation of the surface elevation along the long horizontal section after the transition slope. Results are only shown for α = 1000, 100 and 10 for Case RA2 and Case RD2. In Case RA2, a consistent wave height is observed with no modulations after the 1:1000 transition slope, and only slight modulations after the 1:100 transition slope. However, noticeable small modulations are evident after the 1:10 transition slope. For Case RD2, larger modulations are observed for all transition slopes. For the 1:1000 transition slope, minor modulations are now observed. For the other transition slopes, the modulations become more pronounced, and the wave field shows significant irregularities. Thus, an increase in wave nonlinearity and transition slope increases the modulation of the surface elevation along the horizontal section.

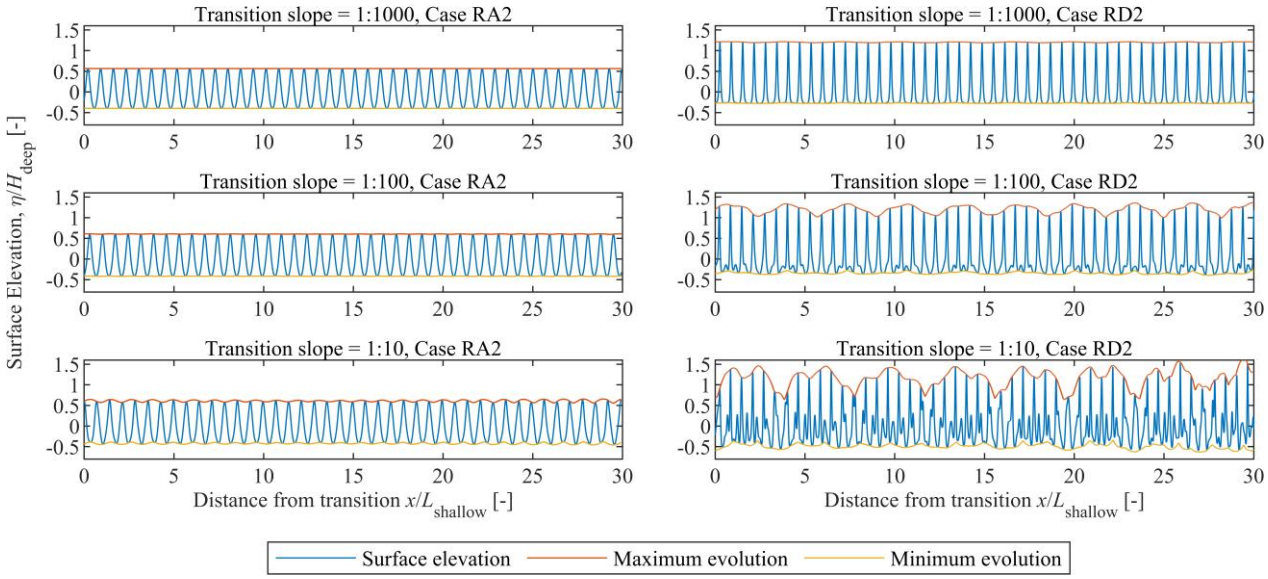

Figure 3. Surface elevation on the horizontal section for Case RA2 and Case RD2.

Figure 4 shows the results of a one-dimensional Fast Fourier Transform (1D FFT) on the surface elevation data in the temporal domain. The FFT is performed for time series in every grid cell along the horizontal section after the transition slope. The figure shows the magnitudes of the primary component as well as the second and third order superharmonics. The standard deviation of these amplitudes for each harmonic is shown in the upper right corner of each plot. Both the amplitudes and the standard deviations are normalised with H_{deep}. The variations in amplitude along the horizontal section explain the modulations observed in the surface elevation shown in Figure 3. In Case RA2, minimal variation is observed for the three harmonics, with only minor variations in the second harmonic for the 1:10 transition slope. For Case RD2, minor variations are observed for the 1:1000 transition slope, while significant variations are observed for all harmonics in the remaining slopes.

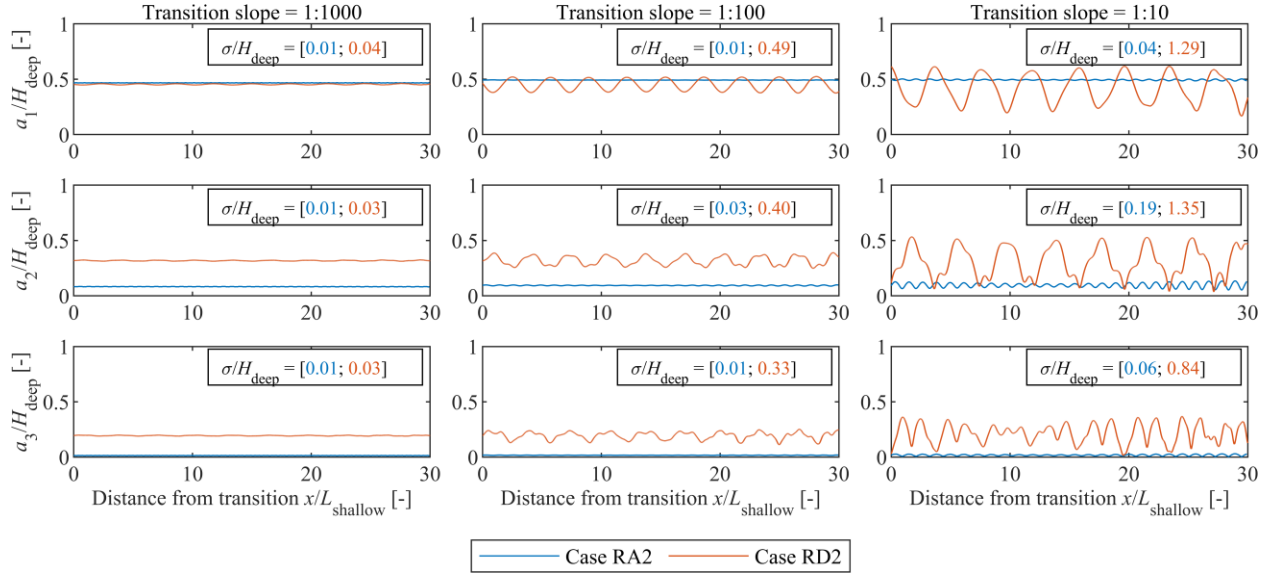

Figure 4. Amplitude of harmonics along the horizontal section.

The variation in amplitudes shown in Figure 4 is caused by multiple components having the same frequency but different wavelengths. One way to extract these wavelengths or wavenumbers at the different frequencies is to use a two-dimensional Fast Fourier Transform (2D FFT). The 2D FFT is applied to the surface elevation data in the temporal and spatial domain along the horizontal section after the foreshore. Figure 5 shows the spectral density as a function of frequency and wavenumber. The textbox shows the ratio of released energy E_{free} to total energy E_{total} for each harmonic, where the free energy has wavenumbers that are not multiples of the primary wavenumber at f_1 and lie outside the black lines. The total energy is the entire energy for the given frequency. The figure shows that Case RA2 with a 1:1000 transition slope has no free energy for f_1 and f_2 while there is 1% free energy at f_3. For the 1:10 transition slope, there is 7% free energy at f_2 and 19% free energy at f_3, but it should be noted that the energy at that frequency is insignificant compared to the wave height, see Figure 4. For Case RD2 with a 1:1000 transition slope, there is 1% free energy at f_2 and f_3, while a substantial amount of free energy is observed for f_1, f_2 and f_3 in the case of a 1:10 foreshore.

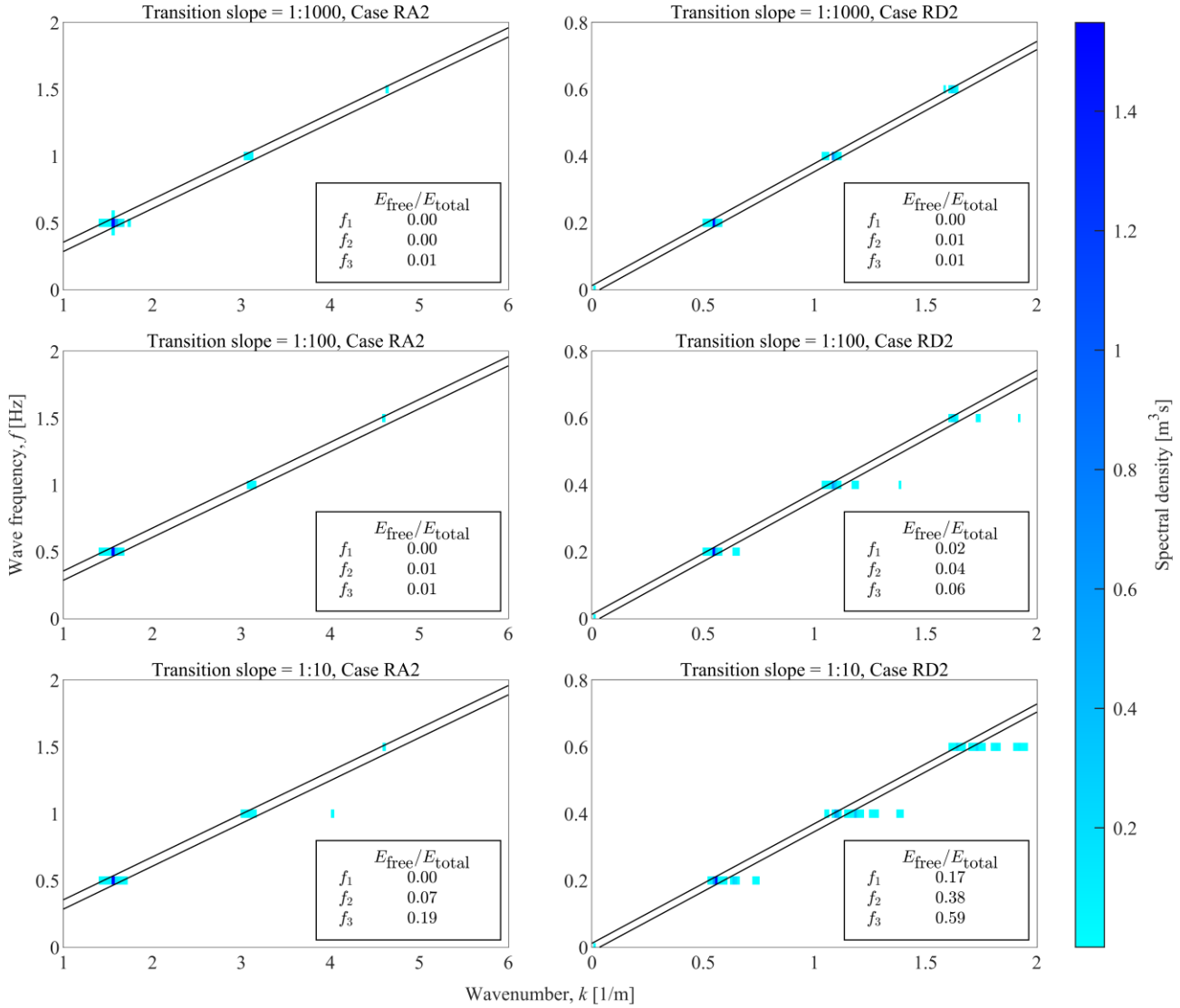

Figure 5. Spectral density as function of wave frequency and wavenumber. The box in each plot shows the ratio E_{free}/E_{total} for the first three harmonics.

For all conducted simulations, the ratio of the total E_{free}/E_{total} for the three harmonics is shown in Figure 6. The figure shows the influence of the transition slope, wave steepness, and relative water depth. It can be observed that waves with low relative water depths at the transition release more free energy than waves with a large relative water depth. Moreover, increasing the wave steepness while maintaining a constant relative water depth, results in a higher release of free energy. The gentlest transition slope of 1:1000 shows less than 1% of the energy is released, while the steepest transition slope shows up to a 52% release of free energy. Thus, it can be concluded that waves in shallow water with significant changes in bathymetry slope can lead to a significant amount of energy being released.

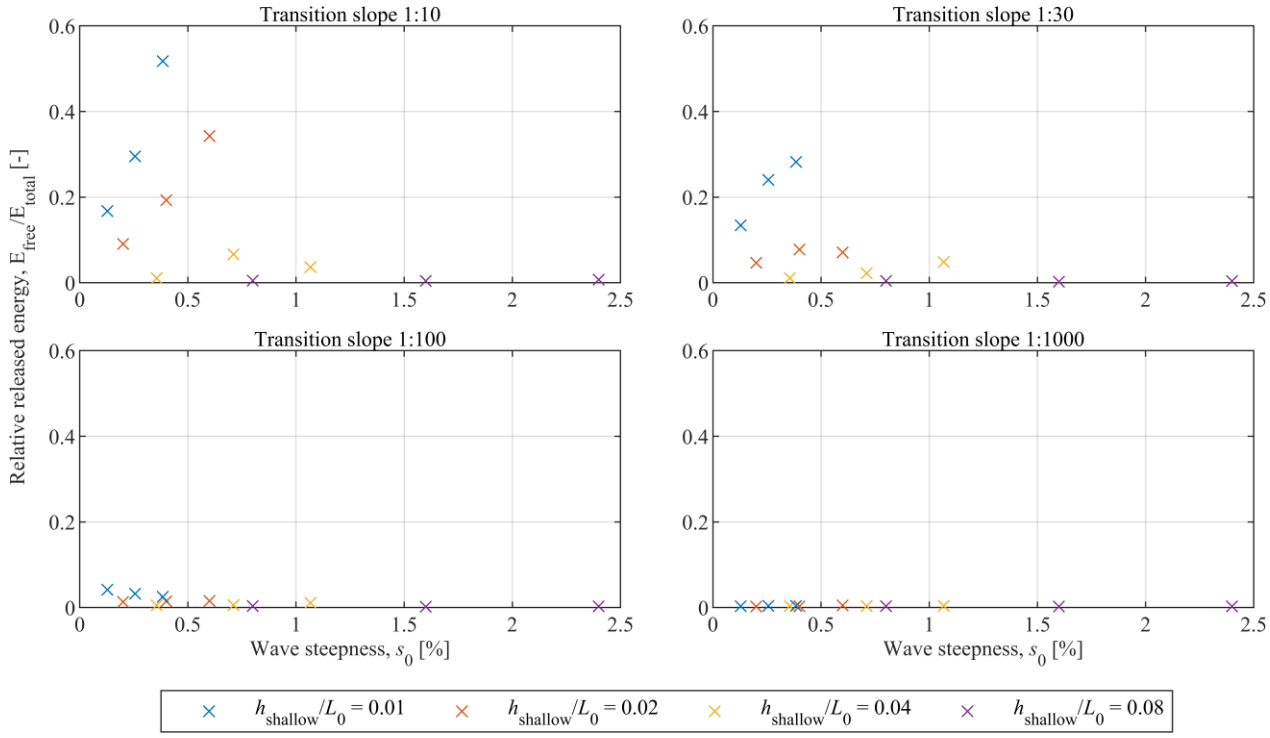

Figure 6. Relative amount of free energy released as function of wave steepness, relative water depth and transition slope.

The free wave energy that is released may lead to generation of freak waves, see Trulsen (2018). He describes that a sudden change in the equilibrium state of the sea causes the release of free waves. The change in the equilibrium might be caused by a sudden change in meteorological conditions, significant changes in currents, bathymetries, or sudden appearances of a ship in the wave field. Thus transition slopes may cause free waves and generate large extreme waves when the free waves are in phase with the bound components. Changes in parameters such as atiltness, wave skewness, and the distribution of velocity profile are just some parameters that could indicate that the waves have a new equilibrium state. Adeyemo (1968) describes that the atiltness of the waves increases for steeper seabed slopes and for decreasing relative water depth h/L. On the other hand, the skewness increases as the seabed slope becomes gentler and when h/L decreases. So, when the wave has to make a significant change in one of these parameters due to a different equilibrium state, then free waves are released.

4 IRREGULAR WAVES

The study with regular waves demonstrated how steep transition slopes might generate unwanted free higher harmonic energy. This forms the basis for the present study of irregular waves. Trulsen et al. (2020) conducted physical model tests, where irregular waves shoaled on a foreshore with a slope of 1:3.8, transitioning to a horizontal section. After the foreshore, they observed that both kurtosis and skewness were changed significantly, caused by the generation of free waves. They observed that the free waves lead to the generation of freak waves, which are characterised either by $H > 2H_{1/3}$ or having a crest elevation $\eta_c > 1.2H_{1/3}$. Hence, employing a transition slope in model tests requires careful consideration, as it may generate extreme waves higher than on a uniform slope. The occurrence of such waves could result in inaccurate model response.

New numerical model tests were performed in order to study the release of free waves in an irregular sea state further. The layout of the numerical model is shown in Figure 7. Irregular waves are generated with a relaxation zone with a width of two peak wavelengths $L_{p,deep}$ calculated using linear wave theory with h_{deep} = 1.5 m and the peak wave period T_p. Following the relaxation zone, a horizontal section of $2L_{p,deep}$ was present. From here, two different layouts were employed, one with a uniform foreshore slope and another with a transition slope followed by the foreshore. At the end of the foreshore, there is a horizontal section of two wavelengths $L_{p,shallow}$ calculated using linear wave theory with $h_{shallow}$ = 0.5 m. A sponge layer with a width of $6L_{p,shallow}$ is used to absorb waves at the end of the model. The layout with the transition slope is modeled with transition slopes α = 5, 10, and 20, and transition water depths h_{trans} = 1.25, 1.00, and 0.75 m. The foreshore slopes used in both models are β = 250, 100, 50, and 30. The generated waves have a deep water wave height of $H_{m0,deep}$ = 0.10 m and wave periods of T_p = 2, 3, 4, and 5 s, see Table 2. Approximately 1,000 waves were generated following a JONSWAP spectra with a peak enhancement factor of γ = 3.3. In total, 16 irregular wave simulations with a uniform slope and 144 simulations with a transition slope were performed.

The models utilised a horizontal resolution of $N_{cell} = L_{p,shallow}/\Delta x$ = 200 and a vertical resolution of N_σ = 10 layers. The

variable time step was based on a maximum CFL criterion of 0.8.

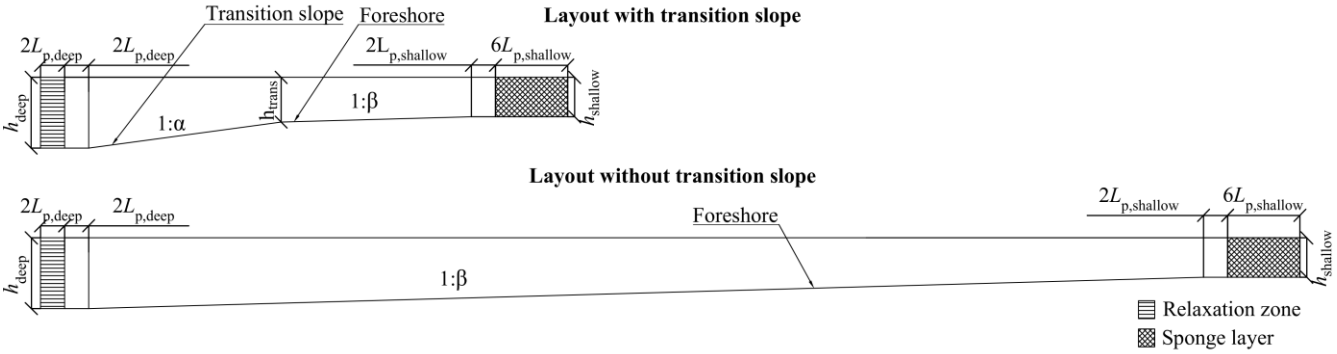

Figure 7. Setup of the numerical wave flume for irregular wave tests.

Table 2 shows the tested wave parameters for each wave case. The waves have a wave steepness from 0.3-1.6% calculated with the wave height at the generation point $H_{m0,deep}$ and the deep water wavelength $L_{0p} = T_p^2 g/(2\pi)$ with g = 9.82 m/s^2. The waves are generated in transitional to shallow water.

Table 2: Irregular wave conditions.

Case	Deep water wave height, $H_{m0,deep}$ [m]	Wave period, T_p [s]	Deep water wave steepness, s_{0p} [%]	Relative water depth at generation, h_{deep}/L_{0p}	Relative water depth at transition, $h_{shallow}/L_{0p}$
IRA	0.10	2	1.6	0.24	0.08
IRB		3	0.7	0.11	0.04
IRC		4	0.4	0.06	0.02
IRD		5	0.3	0.04	0.01

Figure 8 shows the wave spectra for Case IRA and Case IRD at the end of the uniform foreshore and the target wave spectrum at the generation zone. For Case IRA, there are only minor differences between the measured spectra and thus the effect from the foreshore is insignificant. The measured spectra are slightly lower than the target at the generation zone, which can partly be described by a shoaling coefficient close to unity. On the contrary, Case IRD has a notable impact from the foreshore slope, in which a steeper slope has more energy at the peak frequency and less energy at the sub- and superharmonics.

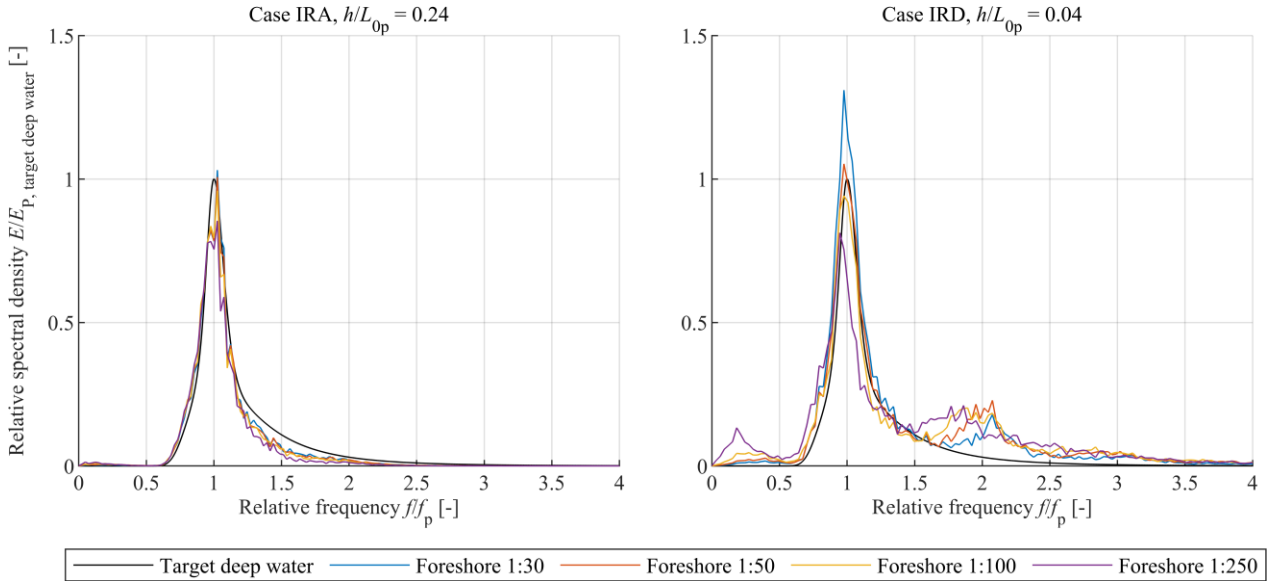

Figure 8. Wave spectra showing the influence of wave steepness and foreshore slope.

The wave transformation along a uniform foreshore is shown in Figure 9. The figure illustrates the shoaling of the spectral wave height H_{m0}, significant wave height $H_{1/3}$, average of the 1/100 wave height $H_{1/100}$, and the transformation of the energy wave period $T_{-1,0}$.

In general, the spectral wave heights demonstrate similar shoaling regardless of the foreshore slope. However, slight deviations are noted on the 1:250 foreshore in Case IRA, and this is judged to be attributed to small numerical damping, which then accumulates over a long distance. $H_{1/3}$ and $H_{1/100}$ show smaller shoaling on the 1:250 foreshore for all wave cases, particularly for the $H_{1/100}$, which is credited to stem from wave breaking that initiates earlier on gentle slopes instead of steep slopes, see Goda (2010). This shows wave steepness has the most significant influence on the shoaling of the waves when they are not breaking due to depth limitation.

The transformation of $T_{-1,0}$ proves to be more sensitive to the foreshore slope than the wave heights. For Case IRA, it is observed that the wave period increases as the waves shoal, with the largest increase on the gentlest slope and the smallest on the steepest slope. As the nonlinearity of the waves increases, the wave period experiences only a slight increase in the deeper part that has been tested, and then it becomes smaller than the initial value in the shallower part, except for the 1:250 foreshore where it only increases. This shows that both wave steepness and foreshore slope significantly influence the transformation of the wave period.

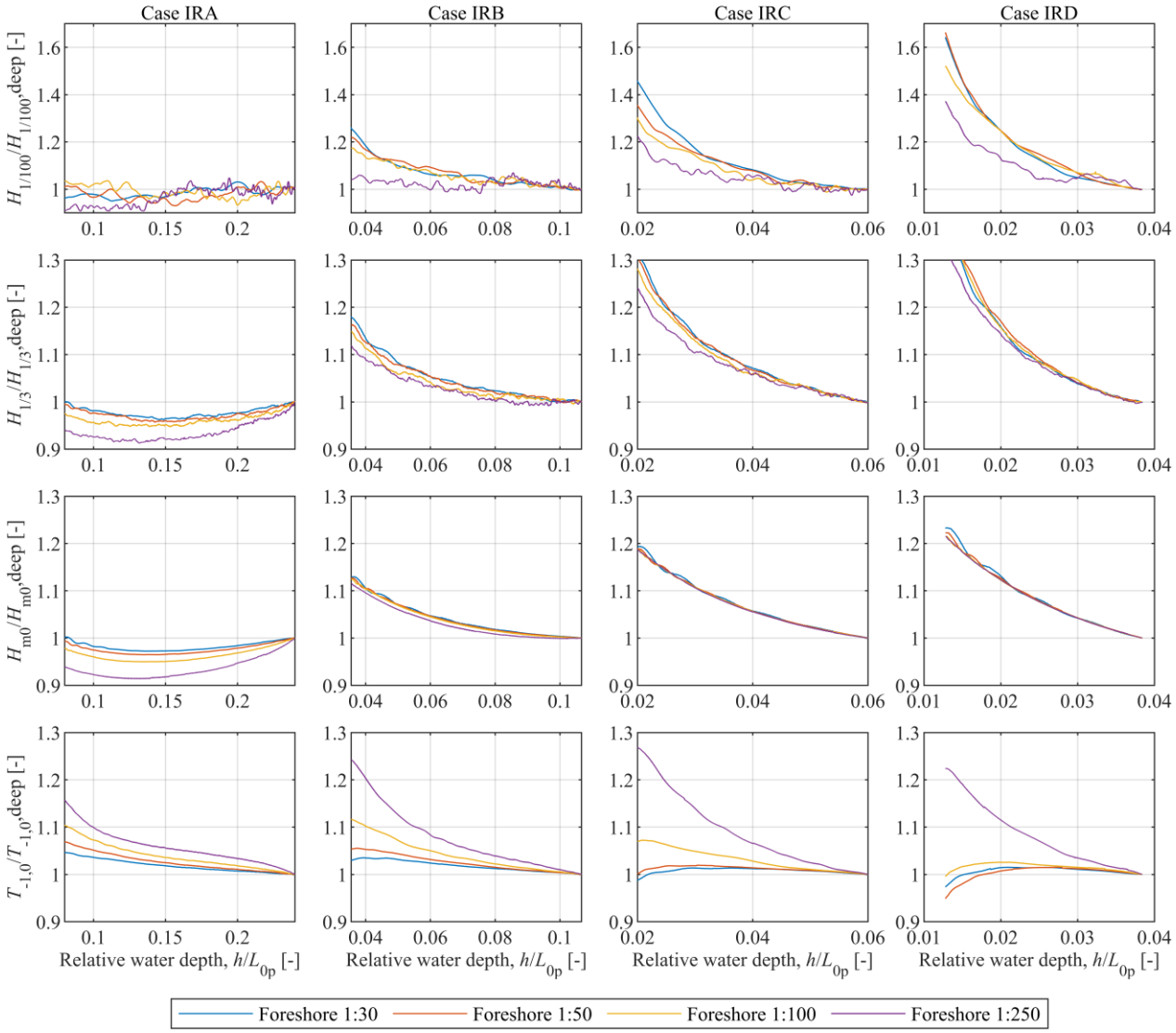

Figure 9. Influence of wave steepness, relative water depth and slope of bathymetry on wave height and wave period transformation.

Figure 10 shows the transformation of $H_{1/100}$, representing the average of the approximately 10 highest waves for the present tests. The $H_{1/100}$ at the different depths is normalised with the $H_{1/100}$ measured before the foreshore for the uniform slope. The black line shows the uniform slope result, while the coloured lines show the results for the different transition

slopes, with the vertical line showing the transition depth between the transition slope and the foreshore. The figure shows that the influence of the transition slope is negligible for Case IRA but substantial for Case IRD. For Case IRD, the $H_{1/100}$ is substantially larger some distance after the transition depth and the effect is largest for h_{trans} = 0.75 m. Figure 10 shows only the results for the 1:10 transition slope, but the deviations are smaller for the 1:20 transition slope, and larger for the 1:5 transition slope.

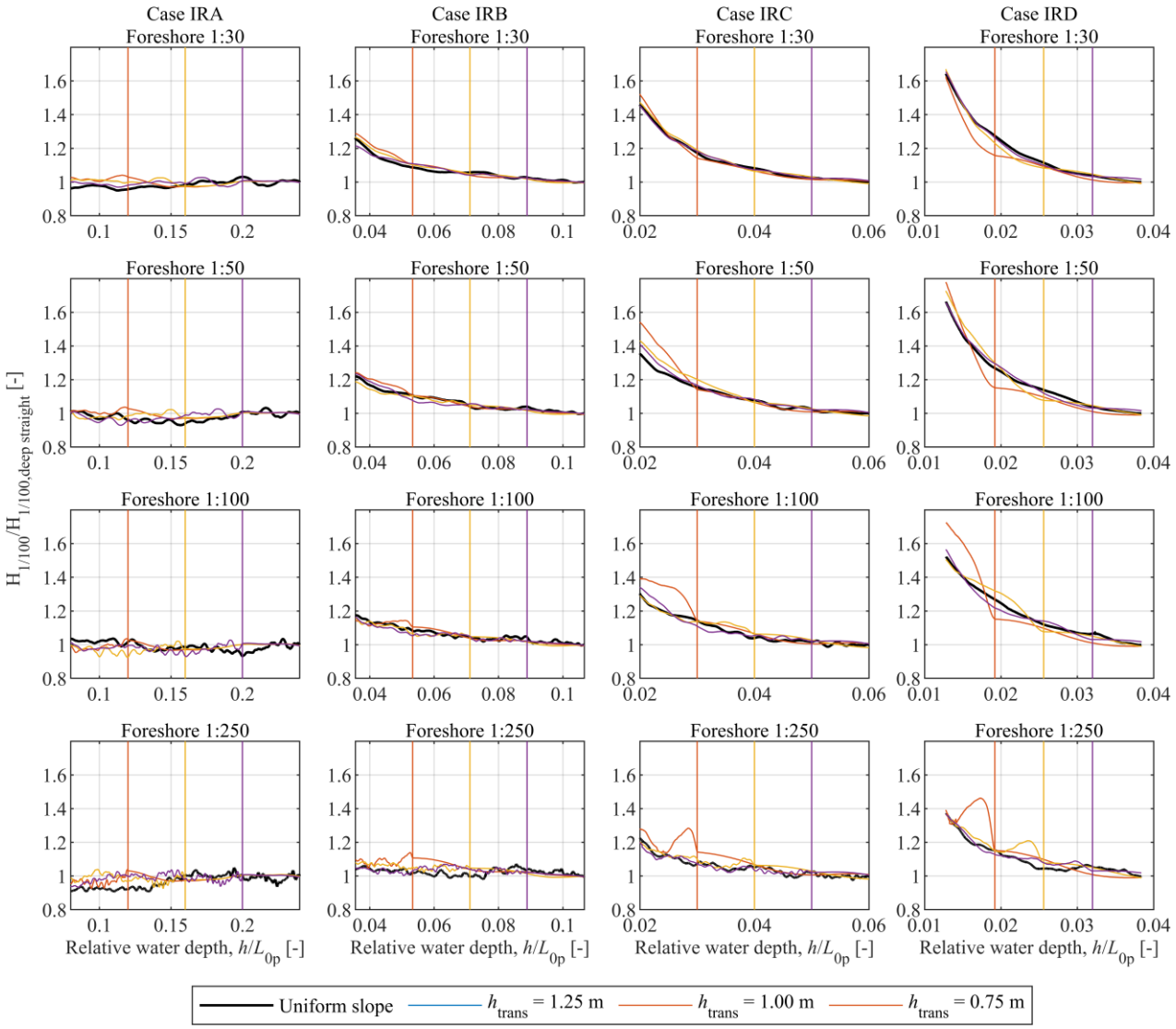

Figure 10. Transformation of $H_{1/100}$ along different foreshore and 1:10 transition slopes. The vertical colored lines show the location for where the transition slope intersects with the foreshore.

Figure 11 shows how the transformation of $T_{-1,0}$ is affected by the transition slope. As observed in Figure 9, the foreshore slope significantly influences the wave period, an influence that is also clear from Figure 11. When the foreshore is steepest, there is no noticeable impact from the transition slope. However, as the foreshore becomes gentler, the influence of the transition slope becomes more pronounced, especially for the most nonlinear Case IRD. Notably, in the case of a gentle foreshore with Case IRA, there is no local minimum, and $T_{-1,0}$ only increases after the transition slope. This suggests that a significant change in bathymetry slope can lead to significant deviations in $T_{-1,0}$ compared to a uniform slope. The deviation of $T_{-1,0}$ increases as h/L_{0p} decreases at the transition depth.

Frostick et al. (2011) suggest having a minimum length of the foreshore that corresponds to 3-5 local wavelengths to ensure proper shoaling and wave breaking. In Case IRD with a 1:250 foreshore, it is evident that the influence of the transition slope, ending at h/L_{0p} = 0.02, is seen for the remaining part of the model. The distance after the transition slope in this configuration is approximately 5 local wavelengths, so within the recommended distance according to Frostick et al. (2011). For Case IRA with a 1:250 foreshore, it is observed that the $T_{-1,0}$ approaches a similar value as the uniform slope at the end of the model. However, the distance for this configuration corresponds to 14 local wavelengths.

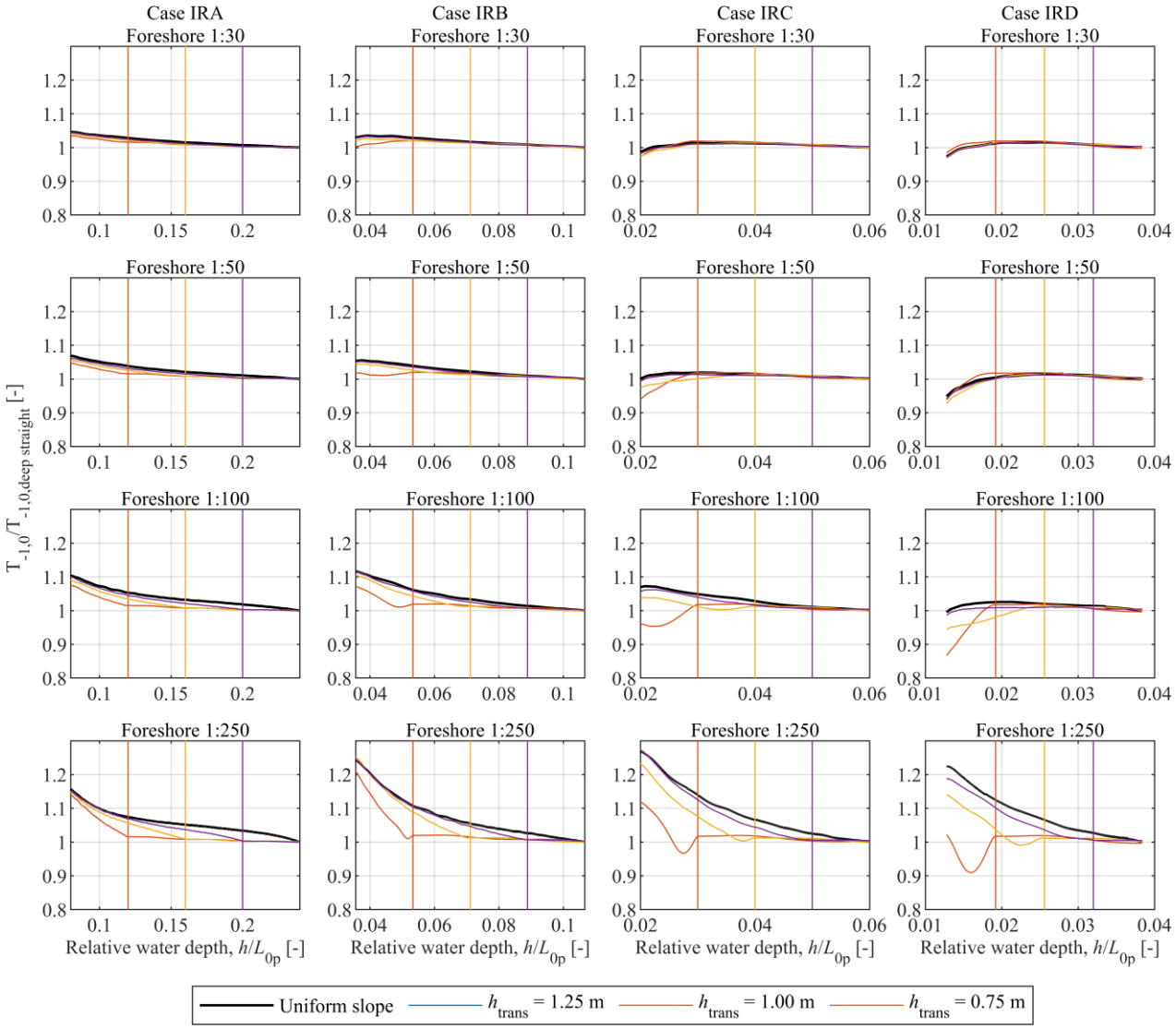

Figure 11. Transformation of $T_{-1,0}$ along different foreshore and 1:10 transition slopes. The vertical colored lines show the location for where the transition slope intersects with the foreshore.

Figure 12 shows the spectra of Case IRA and IRD on the 1:250 foreshore, both with and without a transition slope. The spectra for Case IRA are presented at a depth corresponding to the end of the transition slope, while for Case IRD, they are shown at the depth where the local minimum is identified for $T_{-1,0}$ in Figure 11. In Case IRA, there is an insignificant difference between the spectra with and without the transition slope, with less than 8% deviation in both $T_{-1,0}$ and $H_{1/100}$. For Case IRD, the spectra show significant deviation when a transition slope is applied, leading to reduced subharmonic energy and increased superharmonics energy.

When the free waves are released at the transition depth, the free and bound waves are out of phase. Due to a difference in their celerity, the phase of the free and bound waves will at some distance be in phase and lead to locally high waves. For Case IRD the spectra are shown at a distance of 2.5 local wave lengths L_p after the transition slope. This phenomenon explains the significant presence of superharmonics energy in the spectrum with a transition slope compared to the spectrum with a uniform slope. These free waves contribute to the significant differences in the wave parameters $T_{-1,0}$ and $H_{1/100}$, deviating by 29% and 18%, respectively.

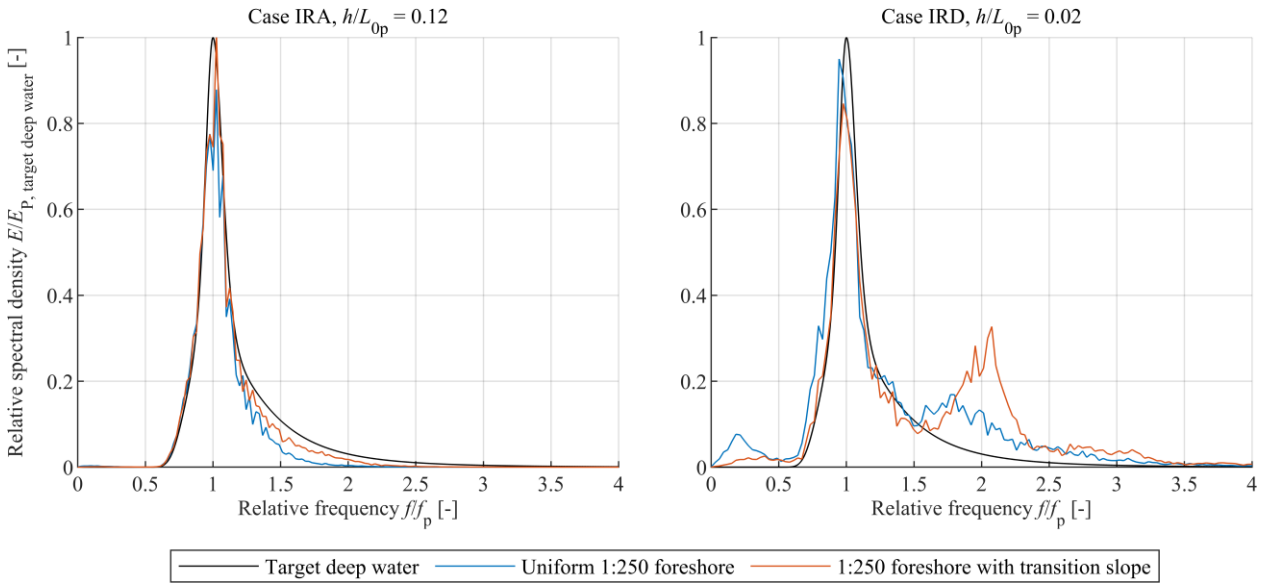

Figure 12. Influence from transition slope on wave spectrum.

In the case of irregular waves, only a single wave height has been modelled for each wave period. Consequently, it is not possible to determine the extent to which the wave steepness affects the release of free waves. However, for the regular waves, it was observed that this factor has a significant influence when the relative water depth is small. In the irregular wave tests, it can be observed that as long as the transition slope ends at $h/L_{0p} > 0.060$ for a foreshore with a slope of 1:250, there is an insignificant influence from the transition slope. For steeper foreshore slopes, such as the 1:30 slope, the transition slope should end at $h/L_{0p} > 0.025$ to have insignificant influence on the wave parameters.

5 CONCLUSIONS

Transition slopes are commonly used in the generation of nonlinear waves in physical models. The purpose is to avoid free waves being generated because of using first- or second-order wavemaker theory in a depth where it is not valid. The effect of these transition slopes on the waves are studied in the present paper by numerical modelling.

Regular wave tests were carried out to illustrate and explain the physical processes occurring as waves propagate from a transition slope to a horizontal section. Several regular waves, characterised by different wave heights and periods, were generated and shoaled on different transition slopes. The regular wave tests revealed that the transition from a steep foreshore to a horizontal seabed resulted in the release of free energy. The equilibrium states of the wave before and after the transition are different, leading to significant variations in the wave parameters such as altitness and skewness. The difference in equilibrium states is the underlying cause of the released free energy. Changes in the slope can induce the generation of free waves, with this effect becoming more pronounced as wave steepness increases and relative water depth h/L decreases. This also means that the more nonlinear the wave is the more pronounced are the free waves released.

For the irregular wave tests, waves were generated with the same H_{m0} but varying T_p. The baseline was a bathymetry with various constant slope angles. These results were compared with models with a transition slope, characterised by different configurations of transition slope angles and relative water depths at the transition point. Results indicated that using a transition slope can significantly modify the wave spectra due to the release of free waves. Just as for the regular waves, the effect is most pronounced when the equilibrium state of the sea undergoes substantial changes. These free waves modify wave parameters, causing deviations from those observed on a uniform foreshore. The presence of these free waves can lead to the generation of freak waves and significant deviations in parameters such as the wave period $T_{-1,0}$ and wave height $H_{1/100}$. The differences between the 1:5, 1:10 and 1:20 transition slopes were found to be minor.

Furthermore, it was observed that these free waves can impact the sea state over a considerable distance, extending up to 14 local wavelengths based on the present numerical results. This distance exceeds the recommended value of 3-5 wavelengths suggested by Frostick et al. (2011). As an alternative, it is proposed to avoid using transition slopes by generating nonlinear waves through a combination of numerical wave models and ad-hoc wave generation. In cases where a transition slope is necessary, it is recommended that, for a foreshore with a slope of 1:250 or flatter, the end of the transition slope should stop at $h/L_{0p} > 0.060$, and for a 1:30 slope, it should stop at $h/L_{0p} > 0.025$. Linear interpolation can be used to determine limits for foreshore slopes falling within the range of 1:250 to 1:30.

REFERENCES

Adeyemo, M. (1968). Effect of Beach Slope and Shoaling on Wave Asymmetry. *Coastal Engineering Proceedings.*

Andersen, J., Eldrup, M. R., Fernandez, G. V., & Ferri, F. (2024). Wave Propagation over a Submerged Bar: Benchmarking of VoF, Sigma Transformation, and SPH Numerical Models against Physical Wave Flume Tests. *Submitted to Discover Applied Sciences*.

Beji, S., & Battjes, J. A. (1993). Experimental investigation of wave propagation over a bar. *Coastal Engineering, 19*(1-2), 151-162.

Beji, S., & Battjes, J. A. (1994). Numerical simulation of nonlinear wave propagation over a bar. *Coastal Engineering*, 1-16.

Eldrup, M. R., & Lykke Andersen, T. (2019). Applicability of Nonlinear Wavemaker Theory. *J. Mar. Sci. Eng., 7*(1).

Eldrup, M. R., & Lykke Andersen, T. (2020). Numerical study on regular wave shoaling, de-shoaling and decomposition of free/bound waves on gentle and steep foreshores. *Journal of Marine Science and Engineering, 8*(5).

Fenton, J., & Rienecker, M. (1980). Accurate numerical solutions for nonlinear waves. *Coastal Engineering Proceedings*, (pp. 50-69).

Frostick, L. E. (2011). *Users Guide to Physical Modelling and Experimentation.* (L. E. Frostick, S. J. McLelland, & T. G. Mercer, Eds.) CRC press.

Goda, Y. (2010). *Random Seas and Design of Maritime Structures* (3rd ed.). World Scientific Publishing Company.

Grue, J. (1992). Nonlinear water waves at a submerged obstacle or bottom topography. *Journal of Fluid Mechanics*, 455-476.

Li, Y., Draycott, S., Zheng, Y., Lin, Z., Adcock, T. A., & van den Bremer, T. S. (2021). Why rogue waves occur atop abrupt depth. *Journal of Fluid Mechanics*.

Orszaghova, J., Taylor, P. H., Borthwick, A. G., & Raby, A. C. (2014). Importance of second-order wave generation for focused wave group. *Coastal Engineering*, 63-79.

Trulsen, K. (2018). Rogue Waves in the Ocean, the Role of Modulational Instability, and Abrupt Changes of Environmental Conditions that Can Provoke Non Equilibrium Wave Dynamics. In M. Velarde, R. Tarakanov, & A. Marchenko, *The Ocean in Motion* (pp. 239-247). Springer, Cham.

Trulsen, K., Raustøl, A., Jorde, S., & Rye, L. (2020). Extreme wave statistics of long-crested irregular waves over a shoal. *Journal of Fluid Mechanics*.

Zhang, H., Schäffer, H. A., & Jakobsen, K. P. (2007). Deterministic combination of numerical and physical coastal wave models. *Coastal Engineering, 54*(2).

Zhang, J., Mendes, S., Benoit, M., & Kasparian, J. (2023). Effect of shoaling length on rogue wave occurrence. *arXiv preprint arXiv:2311.14183 (2023)*.